

See discussions, stats, and author profiles for this publication at: <https://www.researchgate.net/publication/338285630>

# Field-effect passivation of metal/ n -GaAs Schottky junction solar cells using atomic layer deposited Al<sub>2</sub>O<sub>3</sub>/ZnO ultrathin films

Article in *Journal of Vacuum Science & Technology A Vacuum Surfaces and Films* · January 2020

DOI: 10.1116/1.5134773

CITATIONS

3

READS

51

4 authors:



**Amirhossein Ghods**

Missouri University of Science and Technology

28 PUBLICATIONS 80 CITATIONS

[SEE PROFILE](#)



**Vishal Saravade**

Missouri University of Science and Technology

13 PUBLICATIONS 41 CITATIONS

[SEE PROFILE](#)



**Chuanle Zhou**

Northwestern University

45 PUBLICATIONS 154 CITATIONS

[SEE PROFILE](#)



**Ian Ferguson**

Kennesaw State University

435 PUBLICATIONS 5,676 CITATIONS

[SEE PROFILE](#)

Some of the authors of this publication are also working on these related projects:



Atomic ordering in III-V semiconductor alloys [View project](#)



capacitive contacts [View project](#)

# Field-Effect Passivation of Metal/*n*-GaAs Schottky Junction Solar Cells Using Atomic Layer Deposited Al<sub>2</sub>O<sub>3</sub>/ZnO Ultrathin Films

Amirhossein Ghods<sup>1</sup>, Vishal G. Saravade<sup>1</sup>, Chuanle Zhou<sup>1</sup>, Ian T. Ferguson<sup>1,2,a)</sup>

<sup>1</sup>Department of Electrical and Computer Engineering, Missouri University of Science and Technology, Rolla, Missouri 65409

<sup>2</sup>Southern Polytechnic College of Engineering and Engineering Technology, Kennesaw State University, Marietta, GA 30060

a) Electronic mail: ifergus3@kennesaw.edu

In this paper, a novel field-effect passivation technique is used to improve the photovoltaic properties of metal/*n*-GaAs Schottky junction solar cells. In this technique, a relatively large density of positive or negative fixed charges existing at the top surface of the dielectric thin films is used to create an electric field gradient to prevent the photo-generated charge carriers from recombining. Atomic layer deposition (ALD) is used to grow high quality Al<sub>2</sub>O<sub>3</sub> and ZnO ultrathin films used as the passivating materials. Electrical measurements demonstrate an improvement in both diode-like and photovoltaic properties of Schottky solar cells in the proposed stacked Al<sub>2</sub>O<sub>3</sub>/ZnO passivation structure compared to the single Al<sub>2</sub>O<sub>3</sub> layer. This can be attributed to both higher equivalent capacitance/permittivity of the stacked passivation layer and increased density of negative fixed charges at the interface of passivation layer and the semiconductor.

## I. INTRODUCTION

Most of the high-efficiency solar cells are currently based on *p-n* junction rather than Schottky junction structure. A record-high power conversion efficiency of 18.5% is

measured for a single junction graphene/*n*-GaAs Schottky solar cell,<sup>1</sup> which is noticeably lower than the 27.6% observed for the state-of-the-art GaAs *p-n* junction solar cell<sup>2</sup> under the one-sun illumination condition. This can be explained based on thermionic-field emission theory (TFE),<sup>3</sup> where a relatively large reverse saturation current density is observed in metal-semiconductor Schottky junction solar cells compared to *p-n* junction solar cells,<sup>4</sup> mostly due to the lower Schottky barrier height, narrower depletion region width, and larger density of surface states. A higher recombination rate of charge carriers at the surface of the semiconductor or at the interface of the metal-semiconductor junction results in an increase in reverse saturation current density, which subsequently further lowers the Schottky barrier height in these devices.<sup>5</sup> On the other hand, application of the Schottky junction eliminates the need for highly doped wide bandgap semiconductors in the solar cell structure, which can reduce the density of defects that can act as recombination centers.<sup>6</sup> Moreover, the cost-effectiveness of the fabrication process makes the Schottky junction solar cells potentially useful in large-scale photovoltaic device fabrication.<sup>7</sup>

Surface passivation has been shown to be effective in reducing the recombination velocity and improving the photovoltaic properties of solar cells.<sup>8</sup> In this approach, growth of a suitable dielectric material passivates the dangling bonds existing at the surface of the semiconductor. This reduces the density of surface states by minimizing the interface trap density, resulting in a lowered surface recombination rate and reverse saturation current density.<sup>9</sup>

Among different dielectric materials used for passivation purposes, Al<sub>2</sub>O<sub>3</sub><sup>5,10</sup> and ZnO<sup>11</sup> have been widely investigated due to their high-*k* dielectric constant and ability for

high-quality thin-film growth using the atomic layer deposition (ALD) technique. In addition to its passivating properties,  $\text{Al}_2\text{O}_3$  can act as an electron-block/hole-transport layer to decrease the recombination velocity at the interface of the metal-semiconductor in a Schottky junction solar cell.<sup>12</sup> This is mainly due to the large bandgap of  $\text{Al}_2\text{O}_3$  and positioning of the conduction and valence bands. ZnO has also been shown to suppress the growth of the low- $k$  interfacial layer in a metal-semiconductor Schottky junction by increasing the equivalent dielectric constant of the passivation layer.<sup>13</sup>

Field-effect passivation has been introduced as an advancement of the typical surface passivation technique used in the solar cells. In this technique, injection or implementation of a large density of positive or negative fixed charges to the dielectric passivation layer leads to formation of an electric field to repel the photo-generated charge carriers from recombining at the surface of the semiconductor.<sup>14,15</sup> In other words, an electric field is created at the surface of the semiconductor due to a large density of fixed charges that exist at the top surface (within top 2~3 nm) of the dielectric passivation layer.<sup>16</sup> As a result of this, the concentration of charge carriers close to the surface of the semiconductor<sup>17</sup> and the reverse saturation current density in the solar cell are reduced.

$\text{Al}_2\text{O}_3$  with a negative fixed charge density of around  $1.0 \times 10^{12} \text{ cm}^{-2}$  has been widely used as a suitable material for field-effect surface passivation of semiconductors.<sup>16,18,19</sup> Theoretical studies based on density functional theory and hybrid functionals suggest that, on one hand, Al vacancies ( $V_{Al}$ ), Al interstitials ( $Al_i$ ), oxygen interstitials ( $O_i$ ), and oxygen dangling bonds ( $DB_O$ ) can act as fixed charge centers in  $\text{Al}_2\text{O}_3$  thin films grown using the thermal ALD technique.<sup>20,21,22</sup> On the other hand, oxygen vacancies ( $V_O$ ) and Al dangling bonds ( $DB_{Al}$ ) were shown to form charge traps

that can act as recombination centers, which will increase the surface recombination rate and reverse saturation current density.<sup>20</sup> Stacked double-layer Al<sub>2</sub>O<sub>3</sub>/ZnO thin film grown using the ALD technique<sup>23</sup> was shown to be an effective field-effect passivation material for reducing the surface recombination velocity and increasing the carrier lifetime. In this structure, ZnO was shown to reduce the density of charge traps by passivating the As dangling bonds existing on the surface of GaAs.<sup>24</sup> Additionally, the ZnO interlayer can increase the density of the negative fixed charges by formation of the acceptor-like defects, such as Zn vacancies ( $V_{Zn}$ ), oxygen interstitials ( $O_i$ ), and oxygen antisites ( $O_{Zn}$ ).<sup>16</sup>

In this paper, the concept of field-effect passivation is used to improve the photovoltaic performance of metal/*n*-GaAs Schottky junction solar cells. Al<sub>2</sub>O<sub>3</sub> and Al<sub>2</sub>O<sub>3</sub>/ZnO stacks grown using thermal ALD are used as the passivating layer on *n*-GaAs to reduce the leakage current by suppressing the recombination of photo-generated minority carriers. The current-voltage (*I-V*) measurements demonstrate the effectiveness of the field-effect passivation to decrease the reverse saturation current and increase the short-circuit current ( $I_{sc}$ ) and open-circuit voltage ( $V_{oc}$ ) of the Schottky junction solar cells.

## II. EXPERIMENT

The schematic of the processing steps for fabrication of the Schottky junction solar cells is shown in Figure 1.a. Silicon-doped *n*-type GaAs wafers with carrier concentrations of  $6 \times 10^{16} \sim 7 \times 10^{17} \text{ cm}^{-3}$ , thickness of 400  $\mu\text{m}$ , and average etch pit density (EPD) of 5000  $\text{cm}^{-2}$  were purchased from AXT Inc. The samples were first cleaned with acetone and methanol to remove any organic contaminants and subsequently etched in

HCl solution for 60 s to remove the native oxide from the top surface of the *n*-GaAs.<sup>25</sup> A mesa layer was patterned using conventional UV photolithography techniques and etched in H<sub>3</sub>PO<sub>4</sub>:H<sub>2</sub>O<sub>2</sub>:H<sub>2</sub>O (3:1:40 vol.) solution for 120 s at room temperature to create an etch step of 200 nm.

Ohmic contact consisted of a multilayer of Ni/AuGe/Ni/Au<sup>26</sup> (5/100/35/50 nm) and was deposited using the electron-beam evaporation technique at a chamber pressure of  $2 \times 10^{-6}$  Torr. The samples were then annealed using the MILA-5000 rapid thermal annealing system in a forming gas environment (95% N<sub>2</sub> + 5% H<sub>2</sub>) at a temperature of 440 °C for 90 s. Transmission line method (TLM) was used to characterize the electrical properties of the ohmic contact, in which a series of metal-semiconductor junctions were created at various distances relative to each other, and the resistance between each pair of contact is measured by applying external bias voltage to the contacts and measuring the current.<sup>27</sup> The total measured resistance can be plotted versus distance in order to calculate sheet resistance and contact resistivity values. Accordingly, the sheet resistance and contact resistivity were calculated to be 0.13-0.41 Ω/□ and  $3\text{-}5 \times 10^{-3}$  Ω.cm<sup>2</sup>, respectively. Following that, the Schottky collection contact (Ag 5 nm) with equivalent area of 11 mm<sup>2</sup> and its probing pad (Ni/Au 5/100 nm) were similarly fabricated. A chemical pre-treatment step was added prior to Schottky collection metal contact deposition that included a 5 s etch in H<sub>2</sub>SO<sub>4</sub>:H<sub>2</sub>O<sub>2</sub>:H<sub>2</sub>O (1:1:50 vol.) and HCl solutions in order to remove the native oxide layer on the surface of the GaAs and prepare the sample for contact deposition. The cross-section of the final device structure is shown in Figure 1.b. A more detailed description of the fabrication process of the metal/*n*-GaAs Schottky junction solar cells can be found elsewhere.<sup>28,29</sup>

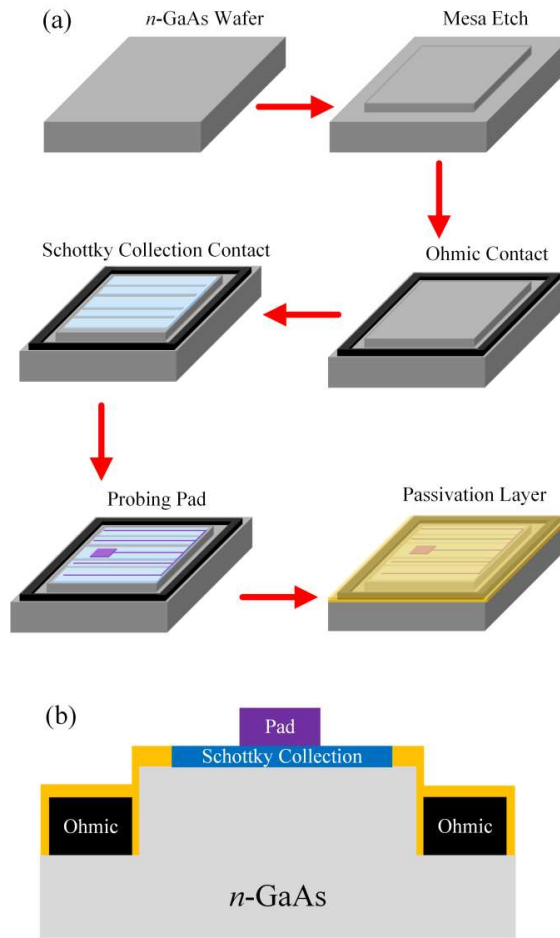


FIG. 1. (a) The schematic of the processing steps for the fabrication of metal/*n*-GaAs Schottky junction solar cells to investigate the effect of field-effect passivation on the photovoltaic properties of the solar cells, (b) cross section of the final device structure.

Two different materials were grown using the ALD technique to investigate their suitability as the passivation layer for the Schottky junction solar cells: I) Al<sub>2</sub>O<sub>3</sub> with trimethylaluminum (TMA) as the metalorganic precursor and II) ZnO with diethylzinc (DEZn) as the precursor. In both growth processes, DI water (DI H<sub>2</sub>O) was used as the oxidizer precursor. These thin films were grown using the GemStar XT thermal ALD

system at a substrate temperature of 200 °C and base pressure of ~50 mTorr, using high purity nitrogen (99.9999%) as the carrier gas with a flow rate of 40 sccm. Table I shows a summary of both growth processes, including the pulse and purge times for each precursor. Ex-situ spectroscopic ellipsometry measurements were performed using a J.A.Woollam ellipsometer at an incident angle of 75° in order to measure the thickness and other optical properties of the grown films. The measurement data were fitted to the Cody-Lorentz optical model, which has been shown to be suitable for amorphous materials.<sup>30,31</sup> Also, the model of the thin films grown on the substrate consisted of a thick (bulk) GaAs substrate without any native oxide (assumed to be removed by HCl and H<sub>2</sub>SO<sub>4</sub> wet etching), and subsequently, the passivation layer (single-layer Al<sub>2</sub>O<sub>3</sub> or double-layer Al<sub>2</sub>O<sub>3</sub>/ZnO) deposited on it. The growth rate per cycle (GPC) for each material was calculated by measuring the total thickness of the grown thin films and dividing it to the total number of cycles. A GPC rate of 1.80 and 1.16 Å/Cycle were observed for ZnO and Al<sub>2</sub>O<sub>3</sub>, accordingly, which is comparable to similar works.<sup>32,33,34</sup>

TABLE I. Summary of the Parameters for ALD Growth of Al<sub>2</sub>O<sub>3</sub> and ZnO.

Material	Precursor	Pulse Time (ms)	Purge Time (s)	Growth Rate Per Cycle (Å/Cycle)
Al <sub>2</sub> O <sub>3</sub>	TMA	20	6	1.16
	H <sub>2</sub> O	20		
ZnO	DEZn	200		1.80
	H <sub>2</sub> O	200		

Two different structures for the passivation layer were studied for this paper and their effect in improving the photovoltaic properties of the metal/*n*-GaAs Schottky solar



cells was investigated. The first structure is based on a 20 nm  $\text{Al}_2\text{O}_3$  layer. The second structure is based on a stacked double-layer  $\text{Al}_2\text{O}_3/\text{ZnO}$  (18/2 nm) configuration, where a 2~3 nm ZnO layer is grown on the  $n$ -GaAs substrate, followed by growth of the 18 nm  $\text{Al}_2\text{O}_3$  top layer. It is expected that the ZnO not only improves the chemical passivation on the surface of  $n$ -GaAs, but also introduces additional negative fixed charges to improve the field-effect passivation properties of the proposed structure. Considering that these negative fixed charges are distributed within the 2~3 nm from the surface, the ZnO layer's thickness has been fixed to be less than 3 nm.<sup>16</sup> It should be noted that the passivation layer with the stacked double-layer  $\text{Al}_2\text{O}_3/\text{ZnO}$  structure was grown in a back-to-back process without any exposure to atmospheric pressure or reduction in substrate temperature between the ZnO and  $\text{Al}_2\text{O}_3$  depositions.

High-resolution transmission electron microscopy (HRTEM) measurements were performed using a FEI Tecnai 20 system, where the images were captured at room temperature at an accelerating voltage of 200 kV. The near-interface structural characterization was done by means of X-ray photoelectron spectroscopy (XPS) using a monochromatic Al-K $\alpha$  X-ray source with energy of 1486.7 eV. In order to ensure that the XPS data for both ZnO and  $\text{Al}_2\text{O}_3$  layers are captured, the samples used for XPS had a thinner  $\text{Al}_2\text{O}_3$  layer thickness of around 3~4 nm, resulting in a total  $\text{Al}_2\text{O}_3/\text{ZnO}$  thickness of 5~6 nm. The calibration process for this spectrum was performed using C 1s spectrum at 284.8 eV as reference in order to correct for the charging.<sup>35</sup> Analysis of the measurement results were performed using CasaXPS software.

The capacitance-voltage ( $C$ - $V$ ) measurements were taken on simplified structures containing  $\text{Al}_2\text{O}_3$  and  $\text{Al}_2\text{O}_3/\text{ZnO}$  on  $n$ -GaAs in order to characterize the effect of

negative fixed charges. The photovoltaic and diode-like properties of the complete Schottky junction solar cells were characterized using current-voltage ( $I$ - $V$ ) measurements, which were performed under the dark and illumination conditions of 1-sun AM1.5G. The forward bias characteristics of the solar cells can be expressed as

$$J = J_0 \exp\left(\frac{qV}{nkT}\right) \quad (1)$$

where  $kT/q$  is the thermal voltage at 300 K and  $J_0$  is the reverse saturation current density, which itself can be represented using Equation (2):

$$J_0 = A^{**}T^2 \exp\left(-\frac{q\phi_{SBH}}{kT}\right) \quad (2)$$

where  $A^{**}$  is the effective Richardson constant ( $8 \times 10^8 \text{ A.m}^{-2}.\text{K}^{-2}$  for  $n$ -GaAs<sup>36</sup>),  $T$  is the absolute temperature in K, and  $\phi_{SBH}$  is the Schottky barrier height in eV. The  $J_0$  can be extracted from the dark  $I$ - $V$  characteristics (not accounting for the photo-generated current) by determining the  $y$ -axis intercept at zero voltage and dividing it to the active device area, followed by calculating the  $\phi_{SBH}$  using Equation (2).<sup>37</sup> Photovoltaic properties of the Schottky solar cells can be calculated from the  $I$ - $V$  characteristics under 1-sun illumination condition.

### III. RESULTS AND DISCUSSION

#### A. Microscopic Interface Characterization

Figure 2.a shows the HRTEM images of the  $n$ -GaAs surface with the stacked  $\text{Al}_2\text{O}_3/\text{ZnO}$  passivation layer. A weak polycrystalline-like structure for the ZnO interlayer and amorphous structure for the  $\text{Al}_2\text{O}_3$  layer were observed. An approximate thickness of

This is the author's peer reviewed, accepted manuscript. However, the online version of record will be different from this version once it has been copyedited and typeset.  
PLEASE CITE THIS ARTICLE AS DOI: 10.1116/1.5134773

2~3 nm for ZnO and 18 nm for the Al<sub>2</sub>O<sub>3</sub> film was measured, confirming the ex-situ ellipsometry measurement results. Moreover, a smooth interface between the passivation layer and *n*-GaAs can be seen, demonstrating the high quality of the ALD-grown thin films. Figure 2.b shows the Zn 2*p* XPS spectrum for the stacked Al<sub>2</sub>O<sub>3</sub>/ZnO layer on the *n*-GaAs, confirming the growth of ultrathin ZnO films.

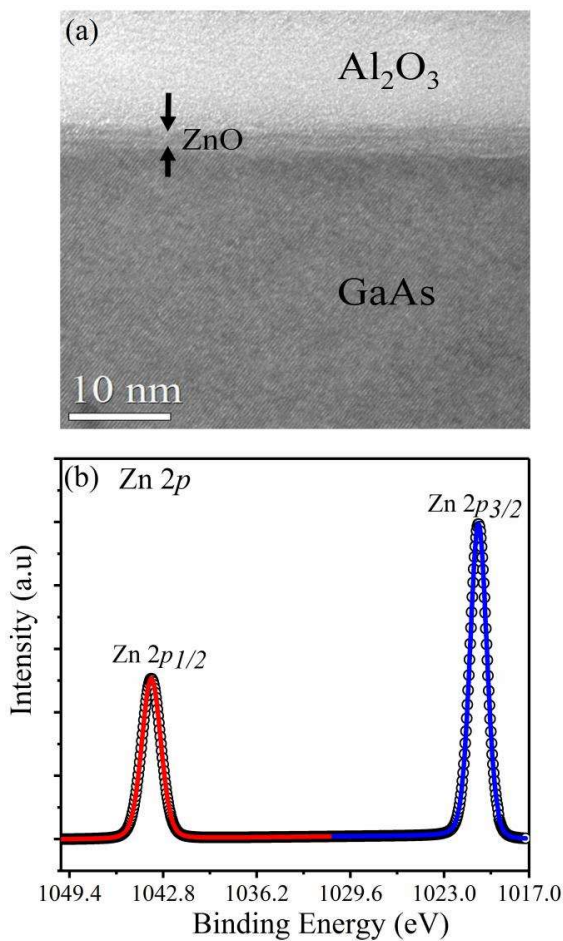


FIG. 2. (a) HRTEM images showing the interface between *n*-GaAs and stacked Al<sub>2</sub>O<sub>3</sub>/ZnO passivation layer, and (b) XPS measurement showing Zn 2*p* spectra in the Al<sub>2</sub>O<sub>3</sub>/ZnO films.

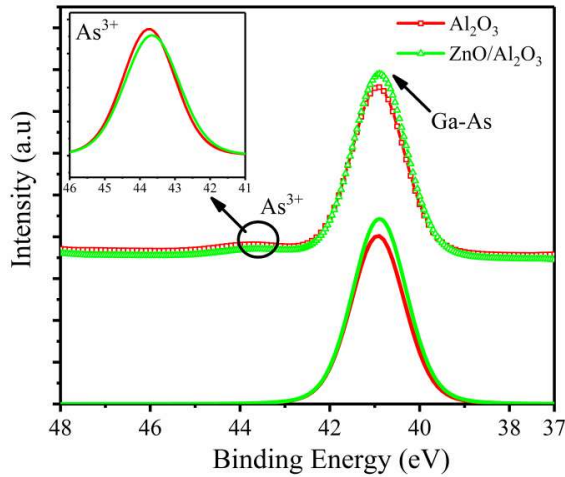


FIG. 3. As 3d XPS spectra obtained from the ALD- $\text{Al}_2\text{O}_3$  and  $\text{Al}_2\text{O}_3/\text{ZnO}$  films grown on GaAs substrate. Fitted peaks represent Ga-As and  $\text{As}^{3+}$  (inset).

### B. Effect of ALD- $\text{Al}_2\text{O}_3$ Passivation Layer

The  $I$ - $V$  characteristics of metal/ $n$ -GaAs Schottky solar cells with and without the 20 nm  $\text{Al}_2\text{O}_3$  surface passivating layer are shown in Figure 4. These measurements were performed under dark condition to extract the diode-like properties, shown in Figure 4.a, and under 1-sun illumination condition to account for the photovoltaic response from these devices, shown in Figure 4.b. The deduced diode-like properties, as shown in Table II, show a reduction in the reverse saturation current density from  $9.0 \times 10^{-9}$  to  $4.5 \times 10^{-11}$   $\text{A}/\text{cm}^2$  and an increase in shunt resistance ( $R_{shunt}$ ) from 8.1 to 10.5  $\text{k}\Omega$ . This could be attributed to a reduction in leakage current due to the higher equivalent capacitance

This is the author's peer reviewed, accepted manuscript. However, the online version of record will be different from this version once it has been copyedited and typeset.  
PLEASE CITE THIS ARTICLE AS DOI: 10.1116/1.5134773

between the metallic contacts caused by the  $\text{Al}_2\text{O}_3$  dielectric thin film. The photovoltaic properties of the Schottky junction solar cells show improvement in  $V_{oc}$  from 173 to 208 mV and  $\phi_{SBH}$  from 770 to 907 meV after passivating with ALD- $\text{Al}_2\text{O}_3$ . Moreover, surface passivation has led to a 51% increase in total generated power from 7.26 to 11.51  $\mu\text{W}$ . These facts can be explained by a reduction in density of surface states, and consequently, reduction in the recombination velocity of minority carriers upon the passivation process.

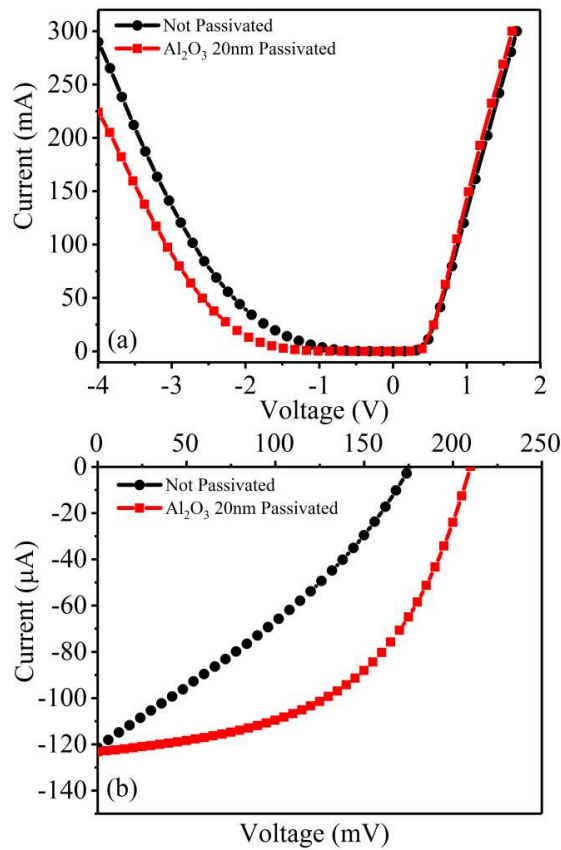


FIG. 4.  $I$ - $V$  characterization showing the effect of a 20 nm ALD- $\text{Al}_2\text{O}_3$  passivation layer on properties of metal/ $n$ -GaAs Schottky solar cells; (a)  $I$ - $V$  measurement under dark condition, and (b)  $I$ - $V$  measurement under 1-sun illumination condition.

A summary of the extracted parameters for the photovoltaic and diode-like properties of metal/*n*-GaAs Schottky solar cells is shown in Table II. A slight improvement in  $I_{sc}$  is observed after Al<sub>2</sub>O<sub>3</sub> passivation, where it increases from 120 to 123  $\mu$ A. This could be attributed to reduction in recombination velocity of photo-generated charge carriers, especially close to the current collection contacts, which leads to improvement in the photo-generated current.

### C. Effect of ALD-Al<sub>2</sub>O<sub>3</sub>/ZnO Passivation Layer

The effect of a 2~3 nm ZnO interlayer in improving the properties of the passivation layer can be understood using the characterization results shown in Figure 5. The C-V characteristics of the devices measured at a frequency of 100 kHz, Figure 5.a, show existence of a strong inversion capacitance at the negative voltages. This could be due to the processing steps, where chemical treatment prior to deposition of the passivation layer would lead to submicron surface inversion of *n*-GaAs.<sup>39,40</sup> Nonetheless, a higher capacitance in both positive and negative voltages for the stacked passivation layer with the ZnO interlayer is observed compared to the Al<sub>2</sub>O<sub>3</sub> structure. Also, the *C-V* measurements show that the capacitance in both voltage ranges increase without reaching to a saturation point, which is likely due to existence of a leakage current. The ellipsometry measurement, shown in Figure 5.b, also shows the stacked passivation layer with a higher permittivity compared to the Al<sub>2</sub>O<sub>3</sub> structure.

A flat-band voltage shift in the positive voltage range was observed in the Al<sub>2</sub>O<sub>3</sub>/ZnO compared to the Al<sub>2</sub>O<sub>3</sub> structure. This decrease in the flat-band voltage indicates an increase in the density of the negative fixed charges in the Al<sub>2</sub>O<sub>3</sub>/ZnO passivation structure, which can be described as<sup>41</sup>

$$N_{fix} \approx \frac{\phi_{SBH} - V_{FB}}{q} \frac{C_{ox}}{A} \quad (3)$$

where  $\phi_{SBH}$  is the Schottky barrier height,  $V_{FB}$  is the flat-band voltage,  $C_{ox}$  is the oxide capacitance, and  $A$  is the Schottky contact area.



This is the author's peer reviewed, accepted manuscript. However, the online version of record will be different from this version once it has been copyedited and typeset.  
PLEASE CITE THIS ARTICLE AS DOI: 10.1116/1.5134773

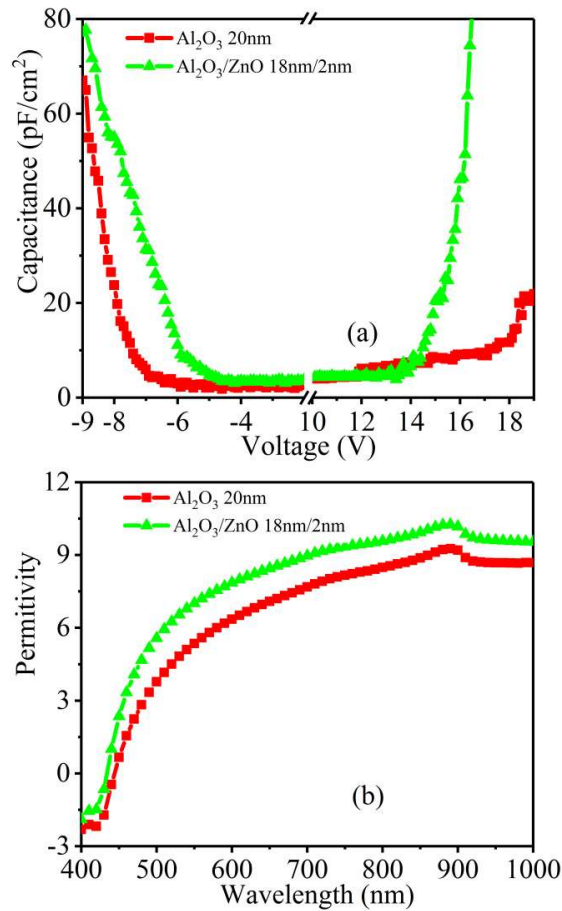


FIG. 5. (a)  $C$ - $V$  characteristics measured at 100 kHz and (b) ellipsometry measurements showing a higher capacitance and equivalent permittivity for the stacked Al<sub>2</sub>O<sub>3</sub>/ZnO layer compared to the Al<sub>2</sub>O<sub>3</sub> structure.

The effect of fixed charges at the dielectric passivation layer plays an important role in reducing the recombination of the charge carriers at the surface of semiconductor. The increase in density of fixed charges, which is caused by the ZnO interlayer, leads to formation of a stronger electric field gradient that repels the charge carriers from nearing the surface of the semiconductor and being trapped.<sup>14</sup> The effect of the ZnO interlayer on photovoltaic properties of the Schottky junction solar cells is depicted in Figure 6, and the deduced diode-like and photovoltaic parameters are shown in Table II. Increases in

$V_{oc}$  from 208 to 398 mV,  $I_{sc}$  from 123 to 148  $\mu\text{A}$ , and efficiency from 0.8% to 2.5% are observed for the stacked  $\text{Al}_2\text{O}_3/\text{ZnO}$  layer compared to the  $\text{Al}_2\text{O}_3$ . Further improvement in the efficiency of our devices is expected by using an anti-reflection coating layer to reduce solar reflection from the top metal contact and optimizing the device structure by adding window and electron/hole blocking layers.<sup>42,43</sup>

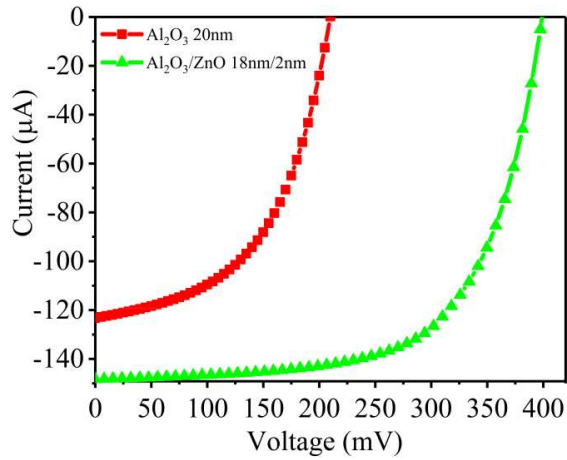


FIG. 6.  $I$ - $V$  measurements for the passivated metal/ $n$ -GaAs Schottky solar cells with only  $\text{Al}_2\text{O}_3$  passivation layer and stacked  $\text{Al}_2\text{O}_3/\text{ZnO}$  passivation layer.

Moreover, a significant reduction in the  $J_0$  from  $4.5 \times 10^{-11}$  to  $1.0 \times 10^{-13}$   $\text{A}/\text{cm}^2$  is observed, indicating the improved passivating properties of the proposed stacked  $\text{Al}_2\text{O}_3/\text{ZnO}$  layer. This can be attributed to induction of additional negative fixed charges and reduction in growth of the As-related oxide layers by using the ultrathin ZnO interlayer. In other words, it would further decrease the concentration of minority carriers at the surface of the semiconductor, reduce the overall recombination velocity, and consequently improves the overall photovoltaic properties of the solar cells.



TABLE II. Extracted Diode-like and Photovoltaic Parameters of the Metal/*n*-GaAs Schottky Solar Cells without and with the two Passivation Structures

	$V_{oc}$ (mV)	$I_{sc}$ ( $\mu$ A)	$\phi_{SBH}$ (meV)	$FF$ (%)	$R_{shunt}$ (k $\Omega$ )	$J_0$ (A/cm <sup>2</sup> )	$P_{max}$ ( $\mu$ W)	$PCE$ (%)
Not Passivated	173	120	769.7	35.0	8.1	$9.0 \times 10^{-9}$	7.3	0.5
Al <sub>2</sub> O <sub>3</sub> Passivated	208	123	907.5	45.0	10.5	$4.5 \times 10^{-11}$	11.5	0.8
Al <sub>2</sub> O <sub>3</sub> /ZnO Passivated	398	148	1066.0	65.0	58.8	$1.0 \times 10^{-13}$	38.2	2.5

#### IV. SUMMARY AND CONCLUSIONS

The effect of field-effect passivation in improving the photovoltaic properties of metal/*n*-GaAs Schottky junction solar cells was studied in this work. Two passivation structures were grown using the ALD technique on the top surface of the solar cells. They include a 20 nm Al<sub>2</sub>O<sub>3</sub> and another stacked Al<sub>2</sub>O<sub>3</sub>/ZnO layer with the approximate thicknesses of 18 nm and 2~3nm. *C-V* and ellipsometry measurements show that the ZnO interlayer not only passivates the *n*-GaAs surface more effectively than just the Al<sub>2</sub>O<sub>3</sub>, but also helps to create an electric field gradient to repel the photo-generated charge carriers by introducing additional negative fixed charges. Moreover, the *I-V* measurements demonstrate an improvement in both diode-like and photovoltaic properties of the Schottky junction solar cells with the use of the Al<sub>2</sub>O<sub>3</sub>/ZnO passivation layer. Notably, the significant reduction in reverse saturation current density confirms the decline in the recombination of the charge carriers, which can be attributed to the field-effect passivation properties of the proposed structure.

## ACKNOWLEDGMENTS

*This research was carried out by financial support from Columbus Photovoltaics, LLC. Authors would also like to acknowledge the technical support received throughout this work from Materials Research Center (MRC) at Missouri S&T in characterizing the ALD-grown thin films and solar cells.*

## REFERENCES

- <sup>1</sup>X. Li, W. Chen, S. Zhang, Z. Wu, P. Wang, Z. Xu, H. Chen, W. Yin, H. Zhong, and S. Lin, *Nano Energy* **16**, 310 (2015)
- <sup>2</sup>B. M. Kayes, H. Nie, R. Twist, S. G. Spruytte, F. Reinhardt, I. C. Kizilyalli, and G. S. Higashi, *IEEE Photovoltaics Specialist Conference*, Seattle, WA (2011).
- <sup>3</sup>F. A. Padovani and R. Stratton, *Solid-State Electron.* **9**, 695 (1966).
- <sup>4</sup>H. S. Kim, M. S. Park, S. H. Kim, S. I. Park, J. D. Song, S. H. Kim, W. J. Choi, and J. H. Park, *Thin Solid Films* **604**, 81 (2016).
- <sup>5</sup>A. Turut, A. Karabulut, K. Ejderha, and N. Biyikli, *Mater. Sci. Semicond. Proc.* **39**, 400 (2015).
- <sup>6</sup>A. Ghods, Y. Wang, C. Zhou, N. Lu, and I. T. Ferguson, "A Review of ZnO-based Thin Films, Devices, and Applications", in *ZnO Thin Films: Properties, Performance and Applications*, Nova Publishers (2019).
- <sup>7</sup>C. G. van de Walle and J. Neugebauer, *Braz. J. Phys.*, **26**, 163 (1996).
- <sup>8</sup>A. G. Aberle, *Prog. Photovolt: Res. Appl.* **8**, 473 (2000).
- <sup>9</sup>L. Zhou, B. Bo, X. Yan, C. Wang, Y. Chi, and X. Yang, *Crystals* **8**, 226 (2018).
- <sup>10</sup>W. C. Wang, C. W. Lin, H. J. Chen, C. W. Chang, J. J. Huang, M. J. Yang, B. Tjahjono, J. J. Huang, W. C. Hsu, and M. J. Chen, *ACS Appl. Mater. Inter.* **5**, 9752 (2013).

- <sup>11</sup>S. Zhu, J. Xu, L. Wang, Y. Huang, and W. M. Tang, *J. Semicond.*, **36**, 034006 (2015).
- <sup>12</sup>M. A. Rehman, I. Akhtar, W. Choi, K. Akbar, A. Farooq, S. Hussain, M. A. Shehzad, S. H. Chun, J. Jung, and Y. Seo, *Carbon* **132**, 157 (2018).
- <sup>13</sup>L. C. Liu, Y. M. Zhang, Y. M. Zhang, and H. L. Lu, *Chin. Phys. B*, **22**, 076701 (2013).
- <sup>14</sup>A. G. Aberle, S. Glunz, and W. Warta, *J. Appl. Phys.* **71**, 4422 (1992).
- <sup>15</sup>G. Agostinelli, A. Delabie, P. Vitanov, Z. Alexieva, H. F. W. Dekkers, S. De Wolf, and G. Beaucarne, *Sol. Energ. Mat. Sol. C*. **90**, 3438 (2006).
- <sup>16</sup>K. S. Jeong, S. K. Oh, H. S. Shin, H. J. Yun, S. H. Kim, H. R. Lee, K. M. Han, H. Y. Park, H. D. Lee, and G. W. Lee, *Jpn. J. Appl. Phys.* **53**, 04ER19 (2014).
- <sup>17</sup>D. Suh and W. S. Liang, “Electrical Properties of Atomic Layer Deposited Al<sub>2</sub>O<sub>3</sub> with Anneal Temperature for Surface Passivation”, *Thin Solid Films* **539**, 309 (2013).
- <sup>18</sup>G. Dingemans and W. M. M. Kessels, *J. Vac. Sci. Technol. A* **30**, 040802 (2012).
- <sup>19</sup>D. K. Simon, P. M. Jordan, T. Mikolajick, and I. Dirnstorfer, *ACS Appl. Mater. Inter.* **7**, 28215 (2015).
- <sup>20</sup>M. Choi, A. Janotti, and C. G. Van der Walle, *J. Appl. Phys.* **113**, 044501 (2013).
- <sup>21</sup>V. Naumann, M. Otto, R. B. Wehrspohn, M. Werner, C. Hagendorf, *Energy Proced.* **27**, 312 (2012).
- <sup>22</sup>A. D. Mallaorqui, E. A. Llado, I. C. Mundet, A. Kiani, B. Demaurex, S. D. Wolf, A. Menzel, M. Zacharias, and A. F. i Morral, *Nano Res.* **8**, 673 (2015).
- <sup>23</sup>J. W. Elam and S. M. George, *Chem. Mater.* **15**, 1020 (2003).
- <sup>24</sup>Y. C. Byun, S. Choi, Y. An, P. C. McIntyre, and H. Kim, *ACS Appl. Mater. Inter.* **6**, 10482 (2014).
- <sup>25</sup>Z. H. Lu, F. Chatenoud, M. M. Dion, M. J. Graham, H. E. Ruda, I. Koutzarov, Q. Liu, C. E. J. Mitchell, I. G. Hill, and A. B. McLean, *Appl. Phys. Lett.* **67**, 670 (1995).

- <sup>26</sup>A. T. Sebastian, J. Phys. D: Appl. Phys. **42**, 125104 (2009).
- <sup>27</sup>H. H. Berger, Solid State Electron. **15**, 145 (1972).
- <sup>28</sup>A. Ghods, V. G. Saravade, A. Woode, C. Zhou, and I. T. Ferguson, IEEE Photovoltaic Specialists Conference, Chicago, IL (2019).
- <sup>29</sup>A. Ghods, V. G. Saravade, A. Woode, C. Zhou, and I. T. Ferguson, IEEE Photovoltaic Specialists Conference, Chicago, IL (2019).
- <sup>30</sup>J. Lopez, J. Martinez, N. Abundiz, D. Dominguez, E. Murillo, F. F. Castillon, R. Machorro, M. H. Farias, H. Tiznado, Superlattice Microst. **90**, 265 (2016).
- <sup>31</sup>J. Price, P. Y. Hung, T. Rhoad, B. Foran, and A. C. Diebold, Appl. Phys. Lett., Appl. Phys. Lett. **85**, 1701 (2004).
- <sup>32</sup>E. Guziewicz, I. A. Kowalik, M. Godlewski, K. Kopalko, V. Osinniy, A. Wójcik, S. Yatsunencko, E. Łusakowska, W. Paszkowicz, and M. Guziewicz, J. Appl. Phys. **103**, 033515 (2008).
- <sup>33</sup>Z. Baji, Z. Labadi, Z. E. Horvath, G. Molnar, J. Volk, I. Barsony, and P. Barna, Cryst. Growth & Des. **12**, 5615 (2012).
- <sup>34</sup>J. W. Elam, Z. A. Sechrist, and S. M. George, Thin Solid Films **414**, 43 (2002).
- <sup>35</sup>W. Lu, Y. Iwasa, Y. Qu, D. Jinno, S. Kamiyama, P. M. Peterson, and H. Ou, RSC Adv. **7**, 8090 (2017).
- <sup>36</sup>M. Missous, E. H. Rhoderick, D. A. Woolf, and S. P. Wilkes, Semicond. Sci. Technol. **7**, 218 (1992).
- <sup>37</sup>S. M. Sze and K. K. Ng, “*P-N Junctions*” in *Physics of Semiconductor Devices*, John Wiley & Sons (2006).
- <sup>38</sup>G. Lucovsky and F. L. Galeener, J. Non-Cryst. Solids **37**, 53 (1980).

This is the author's peer reviewed, accepted manuscript. However, the online version of record will be different from this version once it has been copyedited and typeset.  
PLEASE CITE THIS ARTICLE AS DOI: 10.1116/1.5134773

- <sup>39</sup>Y. Xuan, Y. Q. Wu, T. Shen, T. Yang, and P. D. Ye, IEEE International Electron Devices Meeting, Washington, DC (2007).
- <sup>40</sup>P. K. Hurley, E. O'Connor, V. Djara, S. Monaghan, I. M. Povey, R. D. Long, B. Sheehan, J. Lin, P. C. McIntyre, B. Brennan, R. M. Wallace, M. E. Pemble, and K. Cherkaoui, IEEE Trans. Dev. Mat. Re. **13**, 429 (2013).
- <sup>41</sup>K. Henkel, H. Gargouri, B. Gruska, M. Arens, M. Tallarida, and D. Schmeiber, J. Vac. Sci. Technol. A **32**, 01A107-1 (2014).
- <sup>42</sup>S. Yavuz, C. Kuru, D. Choi, A. Kargar, S. Jin, and P. R. Bandaru, Nanoscale **8**, 6473 (2016).
- <sup>43</sup>H. He, X. Yu, Y. Wu, X. Mu, H. Zhu, S. Yuan, and D. Yang, Nano Energy **16**, 91 (2015).